ELSEVIER

Journal of Nuclear Materials 273 (1999) 66–78

journal of nuclear materials

www.elsevier.nl/locate/jnucmat

Hydrogen isotope permeation through and inventory in the first wall of the water cooled Pb–17Li blanket for DEMO

O.V. Ogorodnikova [a], M.A. Fütterer [a], E. Serra [b,*], G. Benamati [b], J.-F. Salavy [c], G. Aiello [a]

[a] *Commissariat à l'Energie Atomique, CEA/Saclay, DRN/DMT/SERMA, F-91191 Gif-sur-Yvette, France*
[b] *ENEA Fusion Division, CR Brasimone, I-40032 Camugnano, Bologna, Italy*
[c] *Alten, F-92100 Boulogne–Billancourt, France*

Received 29 October 1998; accepted 22 December 1998

Abstract

The hydrogen isotope transport through the first wall between plasma and first wall coolant has been investigated. The time dependence of hydrogen isotope permeation through the first wall from plasma into water coolant has been calculated. The hydrogen isotope inventory (both mobile and trapped hydrogen isotopes) in the first wall has been evaluated. The influence of temperature gradient, surface conditions, isotopic effect and trapping in the ion- and neutron-induced defects on the hydrogen isotope permeation and inventory has been considered.

1. Introduction

In the case of controlled fusion by magnetic confinement, as it will occur in the demonstration reactor DEMO, tritium recycling from the first wall (FW) influences plasma exhaust during the discharge, while tritium permeation through the first wall is a cost problem because water detritiation is expensive. Numerical codes have been developed for the calculations of recycling, inventory and permeation of hydrogen isotopes in fusion reactor design concepts [1–5]. Hydrogen isotope permeation and inventory depend strongly on the design of the FW, the material of the FW, surface conditions, intensity of the incident D/T flux impinging the FW and presence of neutron-produced traps. The purpose of the present investigation is to calculate the tritium permeation from plasma to the water cooled circuit of the FW for the DEMO reactor as well as hydrogen isotope inventory in the FW. Calculations of hydrogen permeation from the water coolant into vacuum vessel are also presented. The main design parameters for the water cooled Pb–17Li blanket for DEMO are taken from [6].

2. DEMO geometry

A section of the first wall is shown in Fig. 1 [6]. The FW has a corrugated shape on the plasma side in order to minimise thermal stresses. It is assumed that the FW is represented by $L_1 = 0.3 \times 10^{-2}$ m of the thickness of martensitic steel between plasma and water coolant for the FW; about $L_2 \approx 1.3 \times 10^{-2}$ m between plasma and Pb–17Li breeder; and about $L_3 \approx 0.8 \times 10^{-2}$ m between the water coolant for the FW and Pb–17Li. The incident tritium ion flux on the first wall of DEMO is extrapolated from ITER conditions. The temperature distributions in the FW are taken from [7]. A hydrogen concentration in cooling water of 2 wppm (typical for PWRs to combat the corrosive effects of radiolysis) is assumed [8].

* Corresponding author. Tel.: +39-0534 801 463; fax +39-0534 801 225; e-mail: emanuele@netbra.brasimone.enea.it

0022-3115/99/$ – see front matter
PII: S0022-3115(99)00015-X

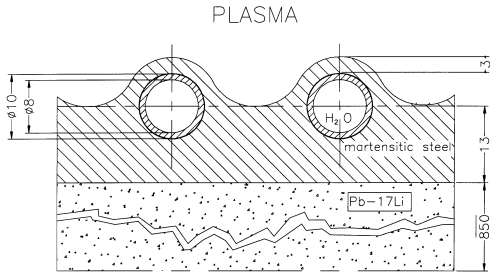

Fig. 1. First wall cross section used in calculations. The lengths are in mm.

3. Model

The hydrogen–solid interaction is usually described by the potential diagram shown schematically in Fig. 2 [9–13]. The mechanisms of penetration of hydrogen molecular gas and hydrogen ions into the metal are different. When hydrogen is absorbed in the bulk of a metal it has to pass through the surface. Experience has shown that hydrogen is not dissolved in the form of molecules but as atoms. In order to penetrate into the bulk, a molecule needs to dissociate into two atoms. For many cases this process is activated. On the other hand, fast atoms and ions penetrate immediately from the plasma into the bulk of the metal without being chemisorbed on the surface. The energetic particles penetrating into the metal slow down in the near surface layer creating defects in the lattice and depositing their energy by electron excitation, atomic displacement and photon excitation.

The randomly migrating hydrogen can become trapped in the defects of the metal. In general, within a solid, various types of traps can be present: vacancies, dislocations, grain boundaries and voids. The trapping process in these particular defect sites influences the retention and diffusion of tritium in the martensitic steel at temperatures below 570 K [14]. The minimum temperature of the water cooled Pb–17Li (WCLL) DEMO first wall is about 612 K [7] and at this high temperature the trapping effects in the lattice defects become negligible for the martensitic 7–10% Cr steels such as T91, F82H, MANET, Batman [14]. For this reason, in this paper, the trapping effects in the usual lattice traps uniformly distributed in the steel are not considered. D/T-ion and He-ion induced defects do not significantly influence the permeation flux but influence the hydrogen isotope retention near the plasma-facing side.

In a fusion reactor, 14 MeV neutrons produce a high damage concentration in the first wall materials. Since the 14 MeV neutrons projected range is much larger than the thickness of the wall, traps are created along the whole wall thickness. For this reason, the defects produced by neutrons may delay the transition permeation flux and strongly influence the hydrogen isotope inventory in the FW. At steady-state, the tritium permeation is not influenced by trapping. Only the time to reach the steady-state may increase by trapping in the neutron- and ion-produced defects.

The transport of hydrogen isotopes through the FW for a dilute solution is described by the diffusion equation:

$$\frac{\partial u_i(x,t)}{\partial t} = \frac{\partial}{\partial x}(J_{\mathrm{d}i}) + I_{0i}^{\mathrm{ion}}\varphi(x) - S_{\Sigma}^{i}(x,t), \quad 0 < x < L, \tag{1}$$

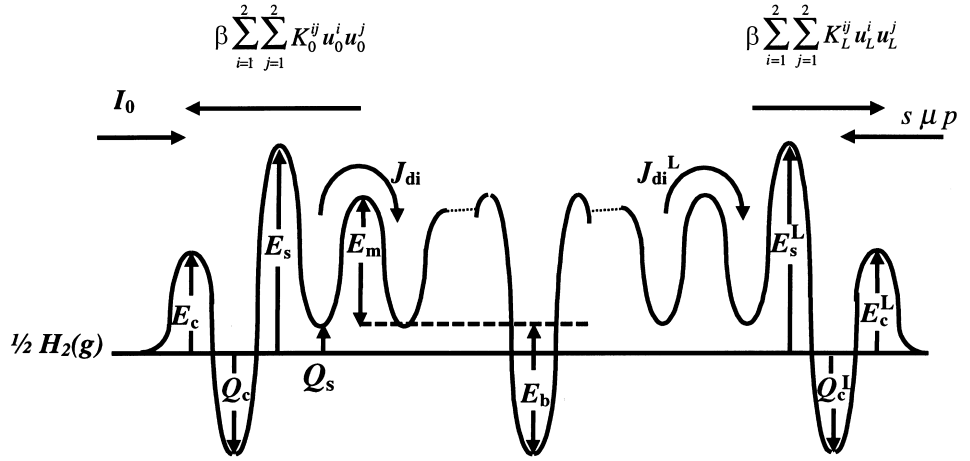

Fig. 2. Schematic diagram of interaction of hydrogen with a metal. Potential relief for hydrogen atom and main fluxes of hydrogen are shown. E_c, Q_c, E_s, Q_s, E_m and E_b are the activation energy for dissociative chemisorption, the heat of chemisorption on the surface, the activation energy for jumps from the chemisorption site on the surface to absorption site in the bulk, the heat of solution, the activation energy for diffusion and the trapping energy, respectively.

where $i = 1, 2, 3$ is the number of diffusing species ($i = 1$ corresponds to hydrogen, $i = 2$ corresponds to deuterium and $i = 3$ corresponds to tritium), $u_i(x,t)$ is the concentration of ith hydrogen isotope in the solute sites of the bulk of the solid, $J_{\mathrm{d}i}$ is the diffusion flux of ith hydrogen isotope and I_{0i}^{ion} is the ion flux of ith hydrogen isotope. The diffusion flux is

$$J_{\mathrm{d}i} = -D_i(\partial u_i/\partial x + (u_i Q/kT^2)\partial T/\partial x), \tag{2}$$

where $D_i = D_{0i}\exp(-E_m/kT)$ is the diffusivity of ith hydrogen isotope, $T(x,t)$ is the temperature and Q is the heat of transport (Soret effect). Experimental measurements of the heat of transport for hydrogen in metals indicate that Q has a weak linear dependence on temperature [15]: $Q = Q_1 + Q_2 T$.

For endothermic metals ($Q_{\mathrm{s}} > 0$), e.g. steels, the hydrogen isotope concentration in the bulk is low and there is no interaction of one isotopic species with another in the bulk of the metal and Eq. (1) is valid.

The $S_{\Sigma}^{i}(x,t)$ is the total rate of filling of the defects by ith hydrogen isotope or ith hydrogen isotope evolution from the defects (several types of defects can exist simultaneously): $S_{\Sigma}^{i}(x,t) = \Sigma_k S_k^i(x,t)$. The ith hydrogen isotope concentration trapped in the defects of the kth type is defined as

$$\partial Y_k^i(x,t)/\partial t = S_k^i(x,t), \tag{3}$$

where $S_k^i(x,t)$ is the sink function for the kth type of defects. The expression for S_k^i can be written as [16]

$$S_k^i(x,t) = R_k D_i\left\{u_i\left[W_k^i - \frac{1}{f_k}\Sigma_{j=1}^{s} Y_k^j\right] - \frac{1}{f_k} Y_k^i z\rho_{\mathrm{Me}}\exp(-E_{\mathrm{bk}}^i/kT)\right\}, \tag{4}$$

where R_k is the radius of the kth trap, z is the number of solution sites per host atom, ρ_{Me} is the density of the metal, f_k is the number of hydrogen atoms that can access the kth trap site, s is the number of species ($s = 3$), E_{bk}^i is the binding energy in the kth type of the defect that is derived as the difference in the potential energy of the atom in normal position in the solution and in the state of binding with the defect (see Fig. 2), $W_k^i = W_k^i(x,t)$ is the concentration of traps (filled plus empty). In this paper, neutron- and ion-induced traps are considered. Neutron-induced traps are distributed along the whole thickness of the sample with concentration W_{n}, while for ion induced defects the concentration of traps at the depth x increases with the ion fluence up to some maximum W_{ion}^m:

$$W_{\mathrm{ion}}^i(x,t) = W_{\mathrm{ion}}^m(1 - \exp(-I_{0i}^{\mathrm{ion}} t\gamma\psi(x,t)/W_{\mathrm{ion}}^m)), \tag{5}$$

where $\gamma\psi(x,t)$ is the rate of defect creation at the depth x.

The ion flux was extrapolated from the ITER conditions $I_0^{\mathrm{ion}} = 3\times 10^{20}$ (atoms m^{-2} s^{-1}) [17]. The ion flux of hydrogen isotopes (50% D and 50% T) incident on the FW from plasma penetrates directly into the bulk of the metal. The diffusion equation for deuterium or for tritium penetrating the solid from the plasma includes the ion source $I_{0i}^{\mathrm{ion}}\varphi(x)$ ($i = 2, 3$). I_{0i}^{ion} in Eq. (1) is the non-reflected fraction of the ith incident ion flux I_{0i}^{ion} on the plasma-facing side and $\varphi(x)$ is the ion source function. In this work, it is assumed that all incident particles I_0^{ion} penetrate into the bulk and $I_{0i}^{\mathrm{ion}} = I_0^{\mathrm{ion}}/2$. If a part of hydrogen isotopes is reflected, the incoming flux becomes $I_{0i}^{\mathrm{ion}} = (I_0^{\mathrm{ion}}/2)(1-r)$, where r is the reflection coefficient. The ion source distribution is approximated by a Gaussian function:

$$\varphi(x) = A\exp(-(x-R_{\mathrm{p}})^2/(2\langle\Delta x^2\rangle)), \tag{6}$$

where $A = 1/\int_0^L \exp(-(x-R_{\mathrm{p}})^2/(2\langle\Delta x^2\rangle))\,\mathrm{d}x$, R_{p} and $\langle\Delta x^2\rangle$ are the ion projected range and the variance, respectively.

On the other hand, the 14 MeV neutrons generated by the fusion reactions produce protium (H) due to (n, p) reactions and helium (He) due to (n, α) reactions within the FW. Since the projected range of 14 MeV neutrons is much larger than the FW thickness, the H and He production rates are practically uniform in the FW. The hydrogen transport in the FW is described by Eq. (1) where we use the hydrogen source I_0^{H} instead of the ion source $I_{0i}^{\mathrm{ion}}\varphi(x)$. The hydrogen in MANET produced from the (n, p) reaction was evaluated in [18]: $I_0^{\mathrm{H}} = 2\times 10^{18}$ (atoms m^{-3} s^{-1}). Since this work is concerned with the transport of the hydrogen isotopes in the FW, helium effects due to helium implantation and helium production in the FW by (n, α) reactions are not considered.

In general, the boundary conditions on the front ($x = 0$) and the back ($x = L$) sides consider hydrogen isotope desorption in molecular form and are given by the balances of fluxes:

$$\lambda\partial u_i(x,t)/\partial t = -\beta\Sigma_{j=1}^{s} K_0^{ij} u_i u_j - J_{\mathrm{d}i} - S_{\Sigma}^{i}(0,t)\lambda + I_{0i}^{\mathrm{ion}}\varphi_i(0)\lambda + \beta\Sigma_{j=1}^{s} J_{gij}^{0}, \quad x = 0, \tag{7}$$

$$\lambda\partial u_i(x,t)/\partial t = -\beta\Sigma_{j=1}^{s} K_L^{ij} u_i u_j + J_{\mathrm{d}i} - S_{\Sigma}^{i}(L,t)\lambda + I_{0i}^{\mathrm{ion}}\varphi_i(L)\lambda + \beta\Sigma_{j=1}^{s} J_{gij}^{L}, \quad x = L, \tag{8}$$

where $\beta = 2$ if $i = j$ and $\beta = 1$ if $i \neq j$, $K_{0,L}^{ij}$ is the recombination coefficient for the ith isotope combined with the jth isotope, $(I_0^{\mathrm{ion}})_{D,T} = I_0^{\mathrm{ion}}/2$ and $(I_0^{\mathrm{ion}})_{\mathrm{H}} = 0$, $J_{gij}^{0,L} = 2(k_{\mathrm{ad}}^{0,L})_{ij} p_{ij}$ (atoms m^{-2} s^{-1}) is the ijth hydrogen isotope adsorption flux.

The adsorption coefficient k_{ad} is given by

$$(k_{\mathrm{ad}})_{ij} = s\mu_{ij}\ (\text{molec. m}^{-2}\ \text{s}^{-1}\ \text{Pa}^{-1}) \tag{9}$$

where the quantity μ is defined by the kinetic theory expression $\mu_{ij} = 1/\sqrt{2\pi m_{ij} k_B T}$ (m_{ij} is the mass of the ijth hydrogen molecule and $k_B = 1.38 \times 10^{-23}$ J/K is the Boltzmann constant) and

$$s = s_0 \exp(-2E_c/kT) \tag{10}$$

is the sticking coefficient (E_c (eV), $k = 8.618 \times 10^{-5}$ eV/K).

Eq. (9) together with Eq. (10) can be written in the following form:

$$(k_{ad})_{ij} = s\mu_{ij} = (s_0 \Big/ \sqrt{2\pi m_{ij} k_B T}) \exp(-2E_c/kT). \tag{11}$$

The recombination coefficient for the ith hydrogen isotope combined with the jth isotope is given by [9]

$$K^{ij}_{0,L} = s\mu_{ij}/K_S^2 \ (\text{molec. atoms}^{-2}\ \text{m}^4\ \text{s}^{-1}), \tag{12}$$

where $K_S = K_{S0} \exp(-Q_s/kT)$ is the Sieverts' constant.

For a water cooled FW the boundary condition on the FW/water coolant interface can be written as the condition of equality of the chemical potential:

$$(u_i^{FW})^2/u_i^{H_2O} = (K_S^{FW})^2/K_H, \tag{13}$$

where u_i^{FW} and $u_i^{H_2O}$ are the concentrations of the ith hydrogen isotope in the FW and water, respectively; K_S^{FW} and K_H are the Sieverts' constants of the hydrogen isotope in the FW and Henry's constant in water, respectively.

Using Eqs. (1)–(13) we can derive the hydrogen isotope thermodesorption rate:

$$J_{0,L} = \beta \Sigma_{i=1}^{3} \Sigma_{j=1}^{3} K^{ij}_{0,L} u^i_{0,L} u^j_{0,L} \ (\text{atoms m}^{-2}\ \text{s}^{-1}). \tag{14}$$

It is important to mention that the boundary conditions in Eqs. (7) and (8) are valid when there is *local* equilibrium between hydrogen in the absorption state and hydrogen in the adsorption state. This means that the concentration in the bulk is proportional to the concentration on the surface, $u/n \approx$ const. This approach is not true when local equilibrium between hydrogen in the bulk and hydrogen on the surface is disturbed, for example, when the hydrogen concentration on the surface becomes close to the maximum available concentration, that may take place, for example, at low temperature and high surface barrier.

4. Initial assumptions

The calculations of tritium permeation have been performed by a numerical solution of the system of Eqs. (1)–(14). The IEA (International Energy Agency) martensitic steel heat F82H belongs to the 7–10% Cr martensitic steel class that has undergone some modifications in order to achieve better low-activation characteristics compared to those of MANET. F82H steel was a candidate material for the first wall and structure for the demonstration fusion reactor DEMO. The data of the deuterium solubility and diffusivity in F82H steel are taken from [14]. The tritium and hydrogen extrapolated values for the diffusivity in this steel are defined using the classical diffusion theory

$$D_i/D_j = \sqrt{m_j/m_i}, \tag{15}$$

where i and j are two different hydrogen isotopes.

According to the classical theory, the diffusion coefficient is inversely proportional to the square root of the mass m of the diffusing atom and the activation enthalpy is mass independent. This is approximately true at high temperature. Only at low temperature the quantum effects become important. The average temperature of the DEMO first wall is about 600–700 K. This temperature is high enough to apply the classical theory.

The solubility of hydrogen isotopes in solid is, according to the classical kinetic theory, isotope independent since it is a statistic process. A quantum mechanical treatment of the solubility process shows that isotope effects have to be taken into account only at low temperature [19].

The data for the heat of transport $Q = Q_1 + Q_2 T$ for α-Fe are taken from [20]: $Q_1 = -0.77$ V and $Q_2 = 5.5 \times 10^{-4}$ eV/K. The physical data of the materials, used for the calculations, are presented in Table 1.

The calculations are performed considering a total internal surface of the water tubes $S_W = 785$ m^2 (outboard $S_{WO} = 548$ m^2 and inboard $S_{WI} = 237$ m^2). The following assumptions are used:

1. the flux of incident D/T ions from plasma to the first wall is $I_0^{ion} = 3 \times 10^{20}$ atoms m^{-2} s^{-1} (50% D and 50% T) extrapolated from ITER conditions [17],
2. the implantation depth is $R_p = 5 \times 10^{-9}$ m [17],
3. the pressure of molecular hydrogen gas in the cooling water corresponds to a hydrogen concentration in water of 2 wppm [8] (i.e. at 598 K, it corresponds to a H_2 pressure in water of $p^w_{H_2} = 1.987 \times 10^4$ Pa),
4. the hydrogen source in the FW produced from the (n, p) reaction was evaluated for MANET in [18]: $I_0^H = 2 \times 10^{18}$ (atoms m^{-3} s^{-1}),
5. according to Ref. [7] the temperature distributions in the part $L_1 = 3 \times 10^{-3}$ m of the first wall between

Table 1
Materials data for deuterium-F82H system

Property		Ref.
D_0 (m^2/s)	1.07×10^{-7}	[14]
E_m (eV)	0.144	[14]
K_{s0} (atoms/m$^3\sqrt{\text{Pa}}$)	4.520×10^{23}	[14]
Q_s (eV)	0.278	[14]

plasma and the first wall coolant is: $T = T_0(1 - \alpha x)$, where $T_0 = 741$ K and $\alpha = 58$ (m^{-1}).

The trapping of ion implanted hydrogen isotopes is usually dominated by vacancies for hydrogen isotope concentrations up to several atomic percents [21]. According to [22], the trap concentration for vacancies generated by neutron- and ion-irradiation can be taken as $W_n = W_{ion}^m = 10^{-2} \times \rho_{Me}$ (m^{-3}) (1 at.%), where ρ_{Me} is the metal density. According to [17], the trap concentration caused by neutron-irradiation is $W_n = 10^{-3} \times \rho_{Me}$ $(m)^{-3}$ (0.1 at.%). We calculate the hydrogen isotope transport in the FW using both 1 at.% and 0.1 at.% of traps. The trap binding energy is related to a vacancy trap type and can be taken as $E_b = 0.63$ eV [21,22].

According to Eq. (12) the recombination coefficient is a function of the sticking coefficient s or the adsorption coefficient k_{ad}. The adsorption coefficient k_{ad} was obtained in [23] for the interaction of deuterium with the martensitic steel MANET. Due to the unknown adsorption coefficient of hydrogen and tritium interaction with martensitic steels such as MANET and F82H, we suppose, on the basis of Eq. (11), that

$$(k_{ad})_i/(k_{ad})_j = \sqrt{m_j/m_i}. \quad (16)$$

The plasma-facing surface may be sputter-cleaned during plasma operation. The sticking coefficient for such an extremely clean surface is often close to unity ($s \cong 1$) [24,25]. This means that the adsorption coefficient for a perfectly ideal clean surface is

$$(k_{ad})_i^{clean} = 1/\sqrt{2\pi m_i k_B T} \text{ (molec. m}^{-2}\text{ s}^{-1}\text{ Pa}^{-1}\text{)}. \quad (17)$$

For example, the adsorption coefficient for tritium is $(k_{ad})_{T_2}^{clean} = 3.95 \times 10^{22}$ (molec. m^{-2} s^{-1} Pa^{-1}) assuming the temperature on the plasma-facing side of $T =$ 741 K.

The data of the adsorption coefficient for a bare steel surface (presence of small amounts of impurities on the surface) for deuterium/MANET interaction [23] as well as for a perfectly sputter cleaned surface are presented in Table 2. Using (Eqs. (1)–(17)), numerical calculations of the tritium permeation from the plasma towards water coolant as well as the hydrogen permeation from the coolant into vacuum vessel are performed. The tritium permeation flux is calculated for different surface conditions on the plasma-facing side.

5. Tritium permeation from plasma into the first wall coolant

Tritium implantation from the plasma is responsible for the tritium permeation towards the coolant circuit for the first wall. In this section the influence of different factors on the tritium permeation from the plasma into cooling tubes for the FW is analysed. These factors are: thermodiffusion, neutron-produced traps and surface conditions.

5.1. Effect of thermodiffusion

The diffusion of the atoms through the steel is influenced by the Soret effect, that is the tendency of atoms to move under a temperature gradient. The tritium permeation in the steel as a function of time including the Soret effect $Q < 0$ and without thermodiffusion $Q = 0$ is presented in Fig. 3. The introduction of thermodiffusion decreases the permeation of tritium by about four times. In general, metals with a positive heat of solution $Q_s > 0$, such as Fe, Ni, etc., have a negative heat of transport $Q < 0$ [15]. Since steel is an endothermic hydrogen absorber, the heat of transport Q is negative. In this case, the diffusion to the cold side (water coolant side) decreases and, therefore, the permeation from plasma to water coolant is reduced. The effect of the negative heat of transport $Q < 0$ may lead to 'forced'

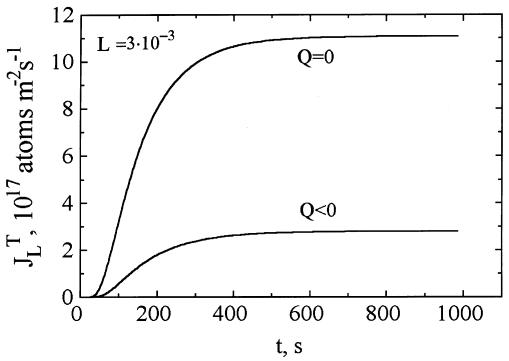

Fig. 3. Time dependence of tritium permeation through a bare steel s^{bare} of the thickness $L_1 = 3 \times 10^{-3}$ m from plasma to the water coolant including thermodiffusion $Q < 0$ and without thermodiffusion $Q = 0$. Ion flux is $I_0^{ion} = 3 \times 10^{20}$ atoms m^{-2} s^{-1}.

Table 2
Data of adsorption and sticking coefficients for deuterium interaction with MANET at different surface conditions

D_2/MANET	k_{ad} (molec. m^{-2} s^{-1} Pa^{-1})	Sticking factor at $T = 741$ K
Bare surface k_{ad}^{bare} [23]	$3.348 \times 10^{17} \exp(-0.198/kT)$	3.1×10^{-7}
Perfectly cleaned surface k_{ad}^{clean} [24,25]	$1.318 \times 10^{24}/\sqrt{T}$	1

hydrogen accumulation near different types of defects, near pores etc., especially in the case of metals with low hydrogen solubility (high $|Q_s|$). It may lead to the degradation of steel.

On the other hand, hydride forming metals, such as Nb, Ti, V, etc. may be expected to have positive heats of transport $Q > 0$, indicating that the temperature gradient will accelerate the transport of tritium to the cold side [15].

5.2. Effect of trapping in neutron produced defects

The influence of the neutron-produced defects on the tritium permeation through the FW is shown in Fig. 4. Trapping in the defects uniformly distributed in the FW can delay the achievement of the steady-state tritium permeation by one order of magnitude but does not influence the steady-state permeation itself.

5.3. Surface effect and discussion

Surface conditions on the plasma-facing side strongly influence the permeation flux. In the calculations we use the adsorption coefficient k_{ad} obtained in [23] for deuterium gas/MANET interaction. During implantation, the adsorption coefficient on the front side of the FW may change because of the cleaning of the surface during the discharge. Both adsorption coefficients for the bare and ideal clean steel surfaces are given in Table 2. The values of the sticking coefficient $s = (k_{ad})_i\sqrt{2\pi m_i k_B T}$ at FW temperature $T = 741$ K are $s^{bare} = 3.1 \times 10^{-7}$ and $s^{clean} = 1$ for a bare and perfectly clean steel surfaces, respectively.

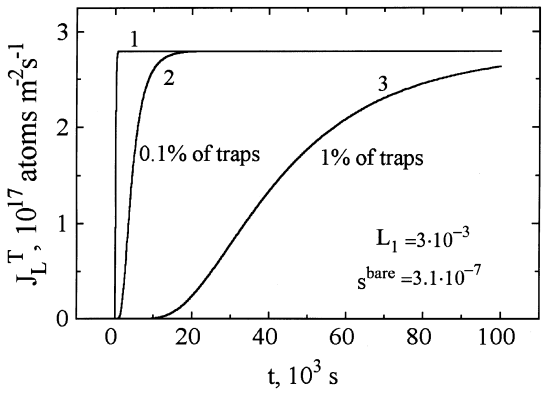

Fig. 4. Influence of neutron-produced defects on tritium permeation through the bare steel s^{bare} of the thickness $L_1 = 3 \times 10^{-3}$ m from plasma into FW water coolant. Curve 1 – without taking into account defects, curve 2 – taking into account neutron-generated defects with 0.1 at.% of traps, and curve 3 – taking into account neutron-generated defects with 1 at.% of traps. Trapping energy is $E_b = 0.63$ eV. Sticking coefficient on the plasma-facing side is $s^{bare} = 3.1 \times 10^{-7}$.

The influence of the Soret effect $T = T_0(1 - \alpha x)$ and surface conditions on the tritium permeation into water cooled tubes from the plasma is presented in Table 3. If the introduction of the thermodiffusion with $Q < 0$ decreases the tritium permeation in water by factor of 3.9, the increase of the sticking coefficient s on the plasma-facing side may reduce the tritium permeation into water by three orders of magnitude. The higher the adsorption constant (or sticking probability) on the front side k^0_{ad} (or s^0), the lower the permeation flux J_L. At steady-state, the tendency is clear: the ion flux equals the sum of the re-emission and permeation fluxes $I^{ion}_{0i} = J^i_0 + J^i_L =$ const. The higher the recombination coefficient, the higher the re-emission flux J_0 and, therefore, the lower the permeation flux J_L. The lowest tritium permeation corresponds to the highest front adsorption coefficient $(k^0_{ad})^{clean}_{T_2}$ or $s = 1$. This becomes obvious if one considers the analytical expression [9] for the steady-state plasma-driven permeation deduced for the diffusion-limited regime

$$(J^{at}_L)^i = (P_i/L)\sqrt{(I^{ion}_0)_i/2(k^0_{ad})_i}, \tag{18}$$

where $P_i = K_S D_i$ is the permeability of ith hydrogen isotope through the steel, L is the thickness of the FW and $(I^{ion}_0)_i$ is the incident ion flux of the ith hydrogen isotope. According to Eq. (11) the relation of the adsorption coefficient with the sticking probability is

$$(k_{ad})_i = s/\sqrt{2\pi m_i k_B T}. \tag{19}$$

It should be noted that Eq. (18) is derived under the assumption that the ion flux I^{ion}_0 slows down just beneath the surface. For a thick sample, like in our case, the ion projected range insignificantly affects the permeation because the diffusion length is much higher than the ion projected range $L_d \approx \sqrt{Dt} \gg R_p$. For this case Eq. (18) is valid. Using Eq. (18) we can roughly evaluate the

Table 3
Influence of the Soret effect $T = T_0(1 - \alpha x)$ and the plasma cleaning until $s = 1$ on the total tritium permeation flux from plasma into water

	All assumptions included	$Q = 0$ without thermodiffusion	$(k^0_{ad})^{clean}$ or $s = 1$ clean surface
Tritium permation flux from plasma to water (atoms m^{-2} s^{-1})	2.79×10^{17}	11×10^{17}	2.19×10^{14}

hydrogen isotope permeation flux through a metal membrane for the diffusion-limited regime without taking into account Soret and isotope effects. According to Eqs. (18) and (19), only the inlet sticking coefficient s is important for a diffusion-limited atomic permeation. With increasing s on the plasma-facing side due to plasma cleaning, the steady-state tritium permeation flux is reduced. For a bare plasma-facing side of the FW, the tritium flux into water is about 24 g/d. However, the tritium permeation into water can be reduced by more than two orders of magnitude with plasma cleaning during implantation (see Table 3). Using Eqs. (18) and (19) we easily find $s \approx 4 \times 10^{-3}$ which corresponds to the assumed limit of 1 g/d for the permeation into the cooling water. Thus, in order to obtain the limit of 1 g/d of tritium into water from ion impingement, the cleaning of the plasma-facing surface until $s \approx 4 \times 10^{-3}$ is necessary. We suggest that the temperature in the FW is uniformly distributed and equals to $T = 741$ K. The Soret effect decreases the permeation flux through the part L_1 of the FW by about four times. Consequently, the tritium permeation through the FW into water from plasma is below 1 g/d if the sticking coefficient is $s \geqslant 10^{-3}$.

Fig. 5 shows the tritium permeation J_L^{T} through the FW towards the water cooled circuit as a function of the sticking coefficient s calculated using Eqs. (18) and (19) (curve 1) and numerically without taking into account thermodiffusion and isotopic effects (curve 2). For high s, the diffusion steps are slow compared to the surface steps. For low s, the surface recombination is the limiting step for the hydrogen isotope permeation. Comparison of curves 1 and 2 allows one to find the sticking factor s^{tr} for the transition from the diffusion-limited regime to the surface-limited one. We can use Eq. (18) for rough estimations of tritium permeation only when the sticking coefficient is higher than $s^{\mathrm{tr}} > 10^{-7}$. When $s^{\mathrm{tr}} < 10^{-7}$, especially in the range of $s^{\mathrm{tr}} < 10^{-9}$, Eq. (18) leads to wrong results. However, such low sticking probability can be observed only for very contaminated or oxidised surfaces [23]. The higher the temperature and thickness of the FW, the lower the sticking probability s^{tr} for the transition from a diffusion-limited regime to a surface-limited one.

Previously, we suggested that the surface may be cleaned during the plasma discharge. The effect of plasma cleaning was observed in [26]. Generally speaking, the surface may be not only cleaned but also contaminated by impurities such as W, Be, C, O and S during plasma operation. It is not clear how the plasma discharge will influence the sticking coefficient s.

The second question that requires a clarification is: how do impurities influence the sticking factor s and, consequently, the recombination coefficient $K_{\mathrm{r}} = s\mu/K_s^2$. In the present study we use the adsorption coefficient $(k_{\mathrm{ad}}^0)^{\mathrm{bare}}$ defined in [23] for deuterium interacted with bare MANET (presence of small amounts of impurities on the surface). The sticking coefficient for a bare steel derived from [23] $s^{\mathrm{bare}} = 6.9 \times 10^{-6} \exp(-0.198/kT)$ is extremely small. A theoretical treatment indicates that

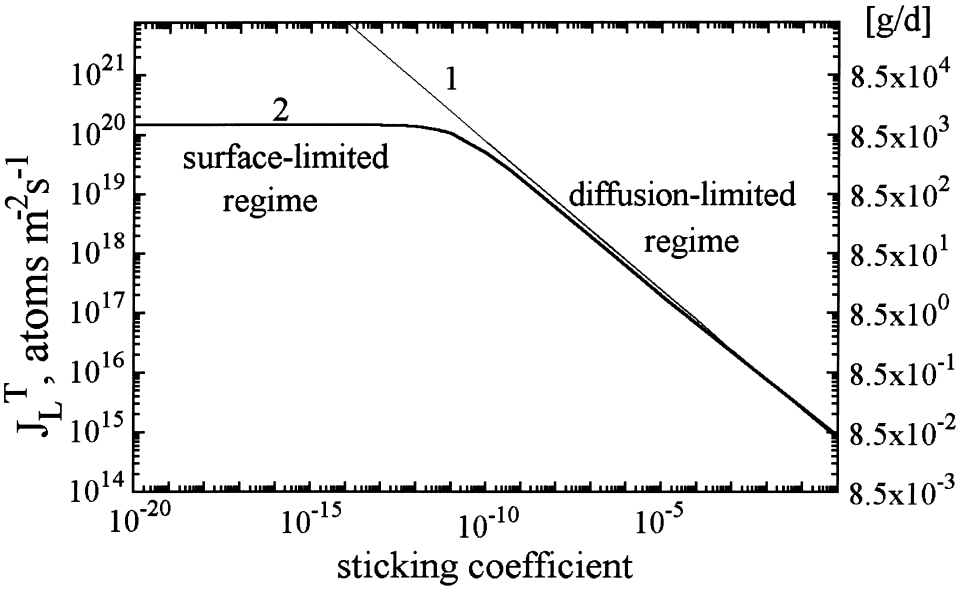

Fig. 5. Tritium steady state permeation flux as a function of sticking probability s. Curve 1 is derived using Eqs. (18) and (19) and curve 2 using numerical calculations. Temperature of the first wall is suggested to be uniformly distributed in the first wall and equals 741 K.

for diatomic molecules, forming an immobile transition complex (α-Fe, MANET), the sticking prefactor is about $s_0 \approx 10^{-4}$ ($s_0 \approx 10^{-5}$ and $s_0 \approx 10^{-3}$ are recommended in [27] and [28], respectively) that is three orders of magnitude higher than measured in [23]. Sticking prefactors $s_0 = 0.16$ and $s_0 = 0.03$ were reported in [29] for α-Fe (1 1 0) and in [30] for α-Fe (1 0 0), respectively. For the same metal the initial sticking coefficient s_0 can widely vary depending on two factors: (i) the structure of the surface (i.e. whether the solid is a single crystal), and (ii) the crystallographic orientation of the surface. The sticking coefficient is quite sensitive to the surface composition. Impurities like O, S or C drastically lower the value of s. The difference in surface conditions can result in a difference of five orders of magnitude in the sticking coefficient of hydrogen on Fe [31]. As it was reported in [21] the experimentally determined recombination coefficient and, consequently, the sticking coefficient, at 400 K range about five orders of magnitude for Fe, six for Ni, four for Pd, and six for stainless steel. Considering the large number of factors which influence the sticking coefficient, it is not surprising that the experimental values of s vary very greatly.

For a clean surface, the sticking coefficient s_0 is a function of structure and crystallographic orientation of the surface. When other gases precover the surface or different chemical elements present on the surface (for example, eroded from the divertor), the sticking coefficient strongly changes. However, the influence of certain impurities on s is unknown. There are only a few papers dealing with the influence of carbon, oxygen and sulfur on the sticking probability. Benziger and Madix [30] studied the effect of these impurities on the hydrogen adsorption on Fe(1 0 0). They measured $s_0^{\text{clean}} = 0.03$ for a clean iron surface. The strongest effect was observed with sulfur. When an Fe(1 0 0)-c(2×2) S surface had been first formed no hydrogen adsorption could be found at all. On an Fe(1 0 0)-p(1×1)O surface at 200 K the sticking prefactor is $s_0 \approx 10^{-4}$ that is two orders of magnitude less than for a clean surface. On an Fe(100)-c(1×1)C surface the sticking prefactor is $s_0 \approx 10^{-3}$ that is also less than s_0^{clean}. In general, the impurities like O, C and S create a surface barrier E_c which drastically decreases the sticking coefficient and, consequently, increases tritium inventory and permeation. For example, E_c was changed from 0.24 eV for 'low carbon: 10%C' to 0.3 eV 'for high carbon: 30%C' surfaces of nickel [32] in experiments of Causey and Baskes [33].

The effect of the alloying element depends on whether it is atomically dispersed on the surface or whether it forms islands. Tungsten or beryllium can co-deposit on the plasma-facing surface with different gases or chemical elements present in the vacuum chamber. Schmidt [34] has investigated the initial sticking probability of hydrogen on a tungsten single crystal. He found s_0 values of 0.25, 0.18 and 0.07 on the (1 1 1), (1 0 0), and (1 1 0) plane, respectively. The sticking coefficient for Be can be evaluated as $s = K_r K_S^2/\mu_D$ ($\mu_D = 1/\sqrt{2\pi m_D k_B T}$), where $K_r = 1.7 \times 10^{-29} \exp(-0.28/kT)$ (m^4/s) is taken from [35]. It is about $s^{\text{Be}} \approx 2 \times 10^{-7} \exp(-0.626/kT)$. If we believe these data, the deposition of tungsten will increase the sticking coefficient and, hence, decrease the tritium permeation, while the deposition of beryllium will reduce s and enhance the tritium permeation. Here, we mean that beryllium and tungsten deposit on the surface as simple impurities but not as a thin layer. In the latter case, tritium diffusion in beryllium and tungsten should be taken into account.

The sticking coefficient might also change due to increasing irradiation defects. However, we should state that the available data are not sufficient to describe the influence of surface impurities and irradiation on the sticking coefficient s.

As already pointed out the sticking probability of hydrogen on steel is expected to be influenced by a large number of effects. During discharge, s can increase and decrease whether cleaning or contamination prevail. As a result, in order to predict the value of s and, consequently, the tritium inventory in and the permeation through the FW, the exact knowledge of the surface conditions during implantation is necessary. In the future more detailed experimental studies to obtain information about the influence of the irradiation on the sticking coefficient have to be carried out.

Due to the lack of reliable data of the sticking probability of hydrogen not only on martensitic steels but also on pure iron, the results presented in this work must be considered only as estimates of the expected behaviour of hydrogen isotope interaction with steel.

6. Hydrogen permeation from the first wall water coolant into the vacuum vessel

To combat the corrosive effects of radiolysis, 2 wppm hydrogen were proposed to be added to the cooling water. The hydrogen pressure $p_{H_2}^{w} = 1.987 \times 10^4$ Pa in the FW water cooled tubes causes the hydrogen permeation flux from the coolant into the vacuum vessel. Hydrogen permeation fluxes from the water coolant into the vacuum vessel are given in Table 4 for different conditions on the plasma-facing side. The conditions on the plasma-facing side are not important for the hydrogen isotope permeation from water into the vacuum vessel. For this reason the hydrogen permeation fluxes from water into the vacuum vessel are similar for a bare and a clean plasma-facing side. The value of the hydrogen permeation flux $J_L^{H} = 3.34 \times 10^{18}$ (atoms m^{-2} s^{-1}) from water coolant into the vacuum vessel is only two orders of magnitude less than the incident deuterium and tritium flux $I_0^{\text{ion}} = 3 \times 10^{20}$ (atoms m^{-2} s^{-1}). The value of the hydrogen permeation flux

Table 4
Hydrogen permeation flux from the FW water coolant into the vacuum vessel for different sticking coefficients s on the plasma-facing side. Calculations are performed considering a total permeation surface of the FW water tubes for the inboard and outboard blanket which is half of the total internal surface of the FW water tubes $S_1 = 392.5$ m^2

	$(k_{ad}^0)^{bare}$	$(k_{ad}^0)^{1g/d}$	$(k_{ad}^0)^{clean}$
	$(s = 3.1 \times 10^{-7})$	$(s = 0^{-3})$	$(s = 1)$
Hydrogen permeation flux (atoms m^{-2} s^{-1}) from water into the vacuum vessel	3.32×10^{18}	3.34×10^{18}	3.356×10^{18}
Hydrogen permeation flux (g/d) from water into the vacuum vessel	283	284	286

from water into the vacuum vessel plasma is about 284 g/d. The consequences for the vacuum pumping system and the isotope separation unit will have to be accounted for.

7. Hydrogen isotope inventory in the first wall

A high hydrogen isotope concentration in the near surface region can be reached due to no-barrier penetration of the incident D/T flux in the steel. Hydrogen trapped in the FW under normal operating conditions can lead to a significant inventory which can degrade the metal properties and can be released during accidents.

The calculated Gaussian profile of implanted deuterium and tritium, and also the profile of ion-induced traps are shown in Fig. 6. Neutron-induced traps are created along the whole wall thickness.

The ith hydrogen isotope concentration in solution sites in the FW near the plasma-facing side can be roughly estimated using the following expression [9]:

$$u_0^i = K_S \sqrt{(I_0^{ion})_i / 2(k_{ad}^0)_i}. \quad (20)$$

The hydrogen isotope concentration in the FW near the water-coolant side is defined by the hydrogen concentration $u_L^{max} = u_L^H$ and can be simply evaluated by the Sievierts law:

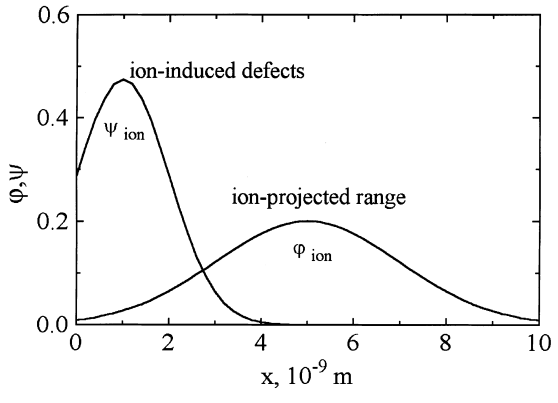

Fig. 6. Calculated implantation profiles.

$$u_L^H = K_S \sqrt{p_{H_2}^w}. \quad (21)$$

At steady-state we can derive the ith hydrogen isotope concentration in defects by the following equation:

$$Y_i = W/(1 + (\exp(-E_b^i/kT) z \rho_{Me}/u_i)), \quad (22)$$

where z is the number of solution sites per host atom, ρ_{Me} is the density of the metal, E_b^i is the trapping energy and W is the concentration of traps (filled plus empty). In Eq. (22) u_i is the ith hydrogen isotope concentration in solution sites in the FW which is equal u_0^i in Eq. (20) for the plasma-facing surface of the FW and u_L^H in Eq. (21) for the water-cooled side.

The hydrogen isotope concentration in the part of the FW between plasma and coolant is given in Table 5 for different sticking coefficients s. An increasing of the sticking factor s strongly reduces the deuterium and tritium inventories in the FW (Fig. 7). For example, for a bare ($s = 3.1 \times 10^{-7}$) steel surface in contact with the plasma the tritium concentration in solution u_T is approximately 10^{23} (atoms m^{-3}) while for an ideally clean ($s = 1$) plasma-facing side it is about 10^{20} (atoms m^{-3}). Unfortunately, the hydrogen concentration $u_H^w \approx 3 \times 10^{23}$ (atoms m^{-3}) on the water coolant side is high due to the high hydrogen pressure in water $p_{H_2}^w = 1.987 \times 10^4$ Pa and does not depend on the surface conditions (see Eq. (21)).

The critical concentration for a hydrogen embrittlement u^* for 9–12% chromium steels is about 4.7×10^{25} atoms m^{-3} (10 wppm) [36]. From Table 5 we can see that the hydrogen isotope concentration in solution u_i does not exceed the assumed limit u^* for any s. However, the influence of irradiation on u^* is unclear until now. The most important hydrogen isotope accumulation can be expected in neutron- and ion-generated traps. The concentration Y_i in traps is one (for 0.1 at.% of traps) or two (for 1 at.% of traps) orders of magnitude higher than that in solution u_i. For a bare $s = 3.1 \times 10^{-7}$ plasma-facing side, the tritium concentration in neutron- and ion-induced traps is $Y_T \approx 10^{25}$ (atoms m^{-3}) for 1 at.% of traps that is below u^*. The increase of s reduces the trapped tritium and deuterium concentrations in the FW. For an ideally clean $s = 1$ plasma-facing side, the maximum tritium trapped concentration is $Y_T \approx 10^{22}$ (atoms m^{-3}) for 1 at.% of traps. With decreasing the

Table 5
Maximum hydrogen isotope concentration in solution u_i, in neutron-produced traps Y_i^n and in ion-produced traps Y_i^{ion} of the part $L_1 = 3 \times 10^{-3}$ m of the FW calculated for different sticking coefficients s on the plasma-facing side. Trap concentration is 1 at.%

Sticking coefficient	$s^{bare} = 3.1 \times 10^{-7}$			$s = 10^{-3}$			$s^{clean} = 1$		
	H	D	T	H	D	T	H	D	T
u_i (atoms m^{-3}) concentration in solutions sites	3.28×10^{23}	3.35×10^{23}	3.7×10^{23}	3.28×10^{23}	6×10^{21}	6×10^{21}	3.28×10^{23}	2.54×10^{20}	2.9×10^{20}
Y_i^n (atoms m^{-3}) 1 at.% neutron-produced traps	1.94×10^{23}	2.98×10^{25}	3.3×10^{25}	1.94×10^{26}	5.75×10^{23}	6.37×10^{23}	1.94×10^{26}	2.45×10^{22}	2.78×10^{22}
Y_i^{ion} (atoms m^{-3}) 1 at.% ion-produced traps	7.4×10^{23}	2.98×10^{25}	3.3×10^{25}	1.4×10^{22}	5.74×10^{23}	6.36×10^{23}	5.3×10^{20}	2.3×10^{22}	2.64×10^{22}
Critical concentration for un-irradiated steel [36]						4.7×10^{25} (atoms m^{-3}) (10 wppm)			

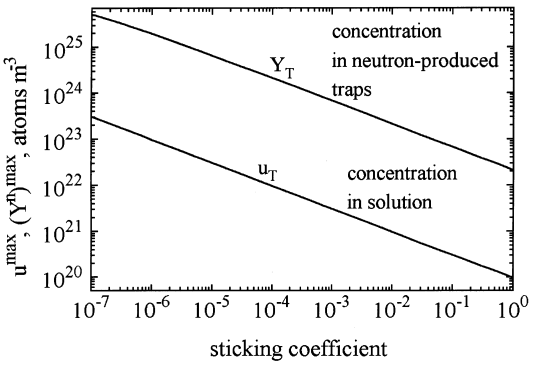

Fig. 7. Maximum tritium mobile u_T and trapped Y_T concentrations in the FW of the thickness of $L_1 = 3 \times 10^{-3}$ m between plasma and the FW coolant as a function of sticking probability s.

trap concentration W by a factor of ten, the hydrogen isotope concentration in traps Y_i decreases also by a factor of ten (see Eq. (22)).

The trapped hydrogen in neutron-produced defects on the water coolant side is $Y_H \approx 10^{26}$ (atoms m^{-3}) for 1 at.% of traps and does not change with s. This value is higher than u^* and can lead to hydrogen degradation of the steel. Thus, the hydrogen addition to the cooling water should be carefully reassessed and adapted to the structural material.

Hydrogen isotope concentration profiles in FW between plasma and the FW water coolant, calculated for mobile u_i and trapped in neutron Y_i^n and ion Y_i^{ion} generated defects, are shown in Figs. 8–10, respectively. As tritium is less mobile than deuterium, the tritium inventory u_T is higher than the deuterium inventory u_D. Hydrogen accumulation in solution sites u_H and in neutron-produced traps Y_H^n is higher than deuterium and tritium because of the high hydrogen pressure $p_{H_2}^w =$

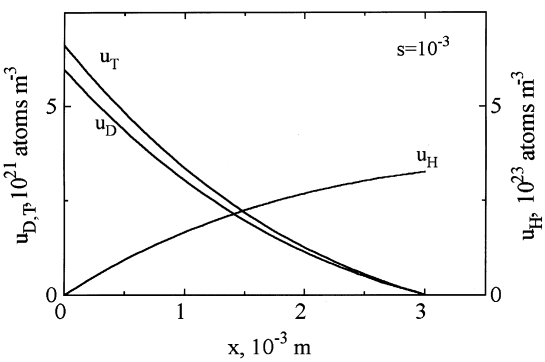

Fig. 8. Hydrogen isotope concentration in solution sites in the part $L_1 = 3 \times 10^{-3}$ m of the FW between plasma and the FW water-coolant as a function of the thickness x. Sticking coefficient on the plasma-facing side is $s = 10^{-3}$.

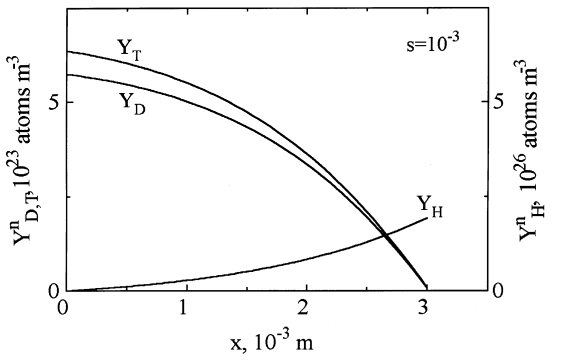

Fig. 9. Hydrogen isotope concentration in neutron-produced traps of the part $L_1 = 3 \times 10^{-3}$ m of the FW between plasma and the FW water coolant as a function of the thickness x. Sticking coefficient on the plasma-facing side is $s = 10^{-3}$.

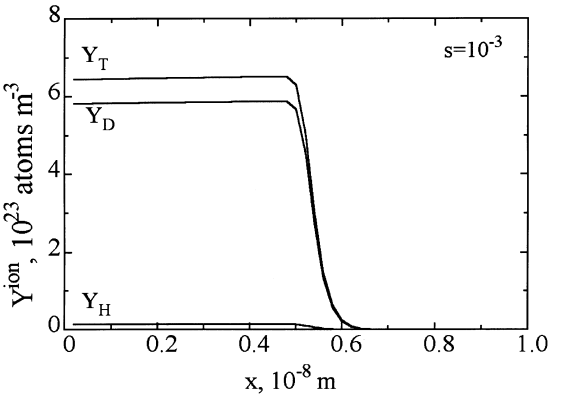

Fig. 10. Steady state hydrogen isotope concentration in ion-induced defects in the FW as a function of the thickness x. Sticking coefficient on the plasma-facing side is $s = 10^{-3}$.

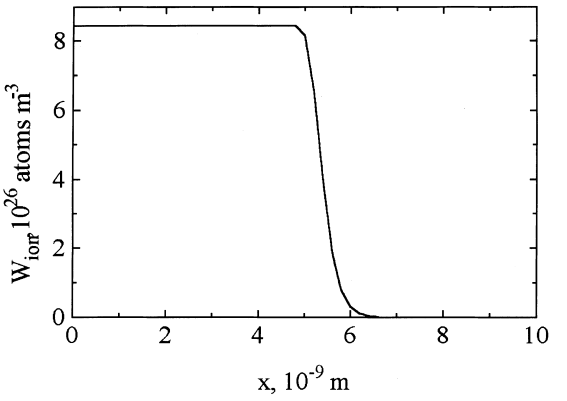

Fig. 11. Steady state concentration W_{ion} of ion-induced defects as a function of the thickness x.

Table 6
Hydrogen isotope inventory in solution u_i and in trap Y_i sites in the part $L_1 = 3 \times 10^{-3}$ m of the FW calculated for the total permeation surface of L_1 for inboard and outboard blanket ($S_w = 392.5$ m^2) using 1 at.% of trap concentration

Sticking coefficient on the plasma-facing sides $s^{\text{bare}} = 3.1 \times 10^{-7}$				$s = 10^{-3}$			$s^{\text{clean}} = 1$		
	H	D	T	H	D	T	H	D	T
Mobile hydrogen isotope inventory u_i [g]	0.33	0.545	0.9	0.33	9.67×10^{-3}	16×10^{-3}	0.33	4.1×10^{-4}	7.04×10^{-4}
Trapped in neutron-produced defects hydrogen isotope inventory Y_i^{n} [g]	122	82.8	136	125	1.568	2.57	125.16	6.65×10^{-2}	11.2×10^{-2}
Trapped in ion-produced defects hydrogen isotope inventory Y_i^{ion} [g]	2.6×10^{-6}	2.124×10^{-4}	3.527×10^{-4}	4.76×10^{-8}	4.16×10^{-6}	6.91×10^{-6}	1.76×10^{-9}	1.5×10^{-7}	2.547×10^{-7}
Total mobile inventory u [g]	1.79			0.33			0.336		
Total trapped in neutron-produced defects inventory Y^{ion} [g]	340.8			129.138			125		
Total trapped in ion-produced defects inventory Y^{ion} [g]	5.65×10^{-4}			1.1×10^{-5}			4×10^{-7}		
Total trapped inventory Y[g] $= Y^{\text{n}} + Y^{\text{ion}}$[g]	340.8			129.138			125		
Total inventory $(u + Y)$ [g]	342			129.5			125.5		

1.987×10^4 Pa in the water coolant. It is important to note that ion generated defects exist only in a thin layer of about 10^{-8} m near the plasma-facing side (Fig. 11). Deuterium and tritium are strongly trapped in ion-produced defects but not hydrogen (Fig. 10) because the hydrogen concentration near plasma-facing side is small: $u_0^{D,T} \gg u_0^H$.

The hydrogen isotope inventory (in gram) in solution and in traps in the part of the FW between plasma and the FW water coolant is presented in Table 6 for different s on the plasma-facing side. The calculations are performed considering a total permeation surface of the water-cooled tubes for the FW (inboard and outboard) which is half of the total internal surface of the water tubes for the FW: $S_w = 392.5$ m^2. Since ion-generated defects are created only in a thin layer near the plasma-facing side, the hydrogen isotope inventory in neutron-produced defects, rather uniformly distributed in the FW, is much higher than in ion-produced defects: $Y_i^n(g) \gg Y_i^{ion}(g)$. Consequently, the total inventory is dominated by the inventory in neutron-produced traps. The total inventory is $(Y+u)^{L_1} = 129$ g for $s = 10^{-3}$ and 1 at.% of traps. The total tritium inventory for the part of the FW between plasma and the FW coolant is given in Table 7 and is about 3 g for $s = 10^{-3}$ and 1 at.% of traps.

Thus, if the plasma-facing side is cleaned during the discharge until $s \geqslant 10^{-3}$, the tritium and deuterium inventories in the FW between plasma and water coolant are below the assumed limit of u^* for both 0.1 at.% and 1 at.% of traps. However, due to the presence of hydrogen in water, for a 1 at.% neutron-produced trap concentration W, there is a high trapped hydrogen concentration of about 10^{26} atoms m^{-3} (for 1 at.% of neutron-produced trap concentration W) on the water-cooled surface which can lead to embrittlement.

8. Conclusions

A model and a computer code for the estimation of the hydrogen isotope permeation through and the inventory in the first wall of the water-cooled lithium-lead (WCLL) DEMO blanket have been developed. The tritium permeation from the plasma through the first wall towards water cooled tubes of the first wall has been calculated. The influence of thermodiffusion, trapping in neutron- and ion-produced defects, and surface conditions on the plasma-facing side has been investigated. Hydrogen permeation from water into vacuum vessel has been also evaluated. The obtained results presented in this report must be considered only as estimates of the expected behaviour due to the unknown surface conditions in the reactor and, consequently, a large uncertainty of the magnitude of adsorption (or sticking) coefficient.

The most important results are:

- The thermodiffusion with negative heat of transport $Q < 0$ decreases the tritium permeation from plasma towards the first wall water coolant by factor of 3.9.
- The plasma-driven permeation is very sensitive to the surface contamination. The adsorption coefficient on the front side of the first wall significantly affects the hydrogen isotope permeation from the plasma into water cooled tubes. The performed calculations are based on the experimental data of the adsorption coefficient obtained by Serra and Perujo [23] for the deuterium gas permeation through a bare (presence of small amounts of impurities on the surface) MANET. It seems that for the bare plasma-facing side the tritium permeation is about 24 g/d that is higher than the assumed limit of 1 g/d. During implantation, the surface of the first wall may be sputter-cleaned and the tritium permeation can decrease by more than two orders of magnitude. The tritium permeation from the plasma towards the cooling water is expected to be below the assumed limit of 1 g/d for the sticking coefficient $s \geqslant 10^{-3}$.
- The contribution of hydrogen in the total inventory of hydrogen isotopes is much higher than deuterium and tritium for the sticking coefficient $s \geqslant 10^{-3}$.
- The hydrogen inventory in the neutron-produced defects is much higher than in ion-produced defects and in solution sites.
- For the sticking coefficient $s = 10^{-3}$, the maximum tritium concentration near the FW/plasma interface in solution sites and in neutron-produced traps with 1 at.% trap concentration are $u_0^{max} = 6.63 \times 10^{21}$ atoms m^{-3} and $Y_0^{max} = 6.57 \times 10^{24}$ atoms m^{-3}, respectively. This means that the tritium concentration is less than the critical concentration for hydrogen embrittlement $u^* = 4.7 \times 10^{25}$ atoms m^{-3} for 9–12%

Table 7
Tritium inventory in solution u_i and in trap Y_i sites in the part $L_1 = 3 \times 10^{-3}$ m of the FW calculated for the total permeation surface of L_1 for inboard and outboard blanket ($S_w = 392.5$ m^2) using 1 at.% of trap concentration

Sticking coefficient	$s^{bare} = 3.1 \times 10^{-7}$	$s = 10^{-3}$	$s^{clean} = 1$
Mobile T inventory [g]	0.9	1.6×10^{-2}	7.04×10^{-4}
Trapped T inventory [g] for 1 at.% of traps	136	2.57	0.112
Total T inventory [g]	136.9	2.57	0.112

chromium steels. The hydrogen concentration in solution sites on the water-coolant side $u_L^{max} = 3.28 \times 10^{23}$ atoms m^{-3} does not exceed the assumed limit u^*. However, a high neutron-induced defect concentration (1 at.% traps) with high trapping energy ($E_b = 0.63$ eV), both lead to a high trapped hydrogen concentration $Y_L^{max} = 1.94 \times 10^{26}$ atoms m^{-3} on the water-cooled surface which can lead to the degradation of the steel. The hydrogen addition to the cooling water should be carefully reassessed and adapted to the structural material.

- The hydrogen permeation flux from water into vacuum vessel is about 284 g/d. The consequences for the vacuum pumping system and the isotope separation unit have to be accounted for.

As already pointed out the sticking probability of hydrogen on the steel is expected to be influenced by a large number of effects. During the plasma discharge, s can increase or decrease depending on surface cleaning or contamination. As a result, in order to predict the value of s and, consequently, the tritium inventory in and the permeation through the first wall, better knowledge of surface conditions during implantation is necessary. In the future the more detailed experimental studies have to be carried out to obtain information about the influence of plasma operation and irradiation on the sticking probability.

Neutron-irradiation effects offer an additional uncertainty. A few data is known on the effect of neutron damage on the trapping of tritium in the plasma-facing metals. There are not available data about trapping energy and concentration of traps produced by 14 MeV neutrons in plasma-facing metals. This is also need a further investigation.

References

[1] M.I. Baskes, SAND 83-8231 (1983).
[2] P. Wienhold, M. Profant, F. Waelbroeck, J. Winter, Jül-1825 (1983).
[3] W. Möller, IPP 9/44 (1983).
[4] G. Gervasini, F. Reiter, J. Nucl. Mater. 155–157 (1988) 754.
[5] G.R. Longhurst, D.F. Holland, J.L. Jones, B.J. Merrill, TMAP4 User's Manual, EGG-FSP-10315, 1992.
[6] L. Giancarli, M.A. Fütterer, Water-cooled Pb-17Li DEMO blanket line. Status report on the related EU activities, CEA report DMT 95/505 (SERMA/LCA/1801), 1995.
[7] J.-F. Salavy, L. Giancarli, L. Baraer, B. Bielak, E. Proust, Water-cooled Pb–17Li blanket: Definition and thermomechanical analysis of the single-box concept, CEA report DMT 93/651, 1993.
[8] M.F. Maday, Fus. Tech. 2 (1996) 1383.
[9] M.A. Pick, K. Sonnenberg, J. Nucl. Mater. 131 (1985) 208.
[10] M.I. Baskes, J. Nucl. Mater. 92 (1980) 318.
[11] P.M. Richards, J. Nucl. Mater. 152 (1988) 246.
[12] T. Nagasaki, R. Yamada, H. Ohno, J. Vac. Sci. Technol. A 10 (1992) 170.
[13] W.M. Shu, Y. Hayashi, K. Okuno, J. Appl. Phys. 75 (1994) 7531.
[14] E. Serra, A. Perujo, G. Benamati, J. Nucl. Mater. 245 (1997) 108.
[15] G.R. Longhurst, J. Nucl. Mater. 131 (1985) 61.
[16] F. Besenbacher, J. Bottiger, S.M. Myers, J. Appl. Phys. 53 (1982) 3536.
[17] L. Berardinucci, M. DalleDonne, Fus. Tech. 2 (1996) 1427.
[18] G. Vella, L. Giancarli, E. Oliveri, G. Aiello, Fus. Eng. Des. 41 (1998) 577.
[19] Y. Ebisuzaki, W. Kass, M. O'Keeffe, J. Chem. Phys. 46 (1967) 1373.
[20] O.D. Gonzales, R.A. Oriani, Trans. TMS-AIME 233 (1965) 1878.
[21] S.M. Myers, P.M. Richards, W.R. Wampler, F. Besenbacher, J. Nucl. Mater. 165 (1989) 9.
[22] B.L. Doyle, D.K. Brice, J. Nucl. Mater. 122/123 (1984) 1523.
[23] E. Serra, A. Perujo, J. Nucl. Mater. 240 (1997) 215.
[24] J.B. Taylor, I. Langmuir, Phys. Rev. 44 (1933) 423.
[25] J.K. Roberts, Proc. Roy. Soc. A152 (1935) 445.
[26] J. Winter, F. Waelbroeck, P. Wienhold, T. Schelske, J. Nucl. Mater. 111/112 (1982) 243.
[27] B.M.W. Trapnell, Chemisorption, Butterworths, London, 1958, p. 94.
[28] D.O. Hayward, B.M.W. Trapnell, Chemisorption, Butterworths, London, 1964, p. 126.
[29] F. Bozso, G. Ertl, M. Grunge, M Weiss, Appl. Surf. Sci. 1 (1977) 103.
[30] J. Benziger, R.J. Madix, Surf. Sci. 94 (1980) 119.
[31] P.L. Andrew, A.A. Haasz, J. Vac. Sci. Technol. A 8 (1990) 1807.
[32] O.V. Ogorodnikova, unpublished.
[33] R.A. Causey, M.I. Baskes, J. Nucl. Mater. 145–147 (1987) 284.
[34] L.D. Schmidt, in: F. Ricca (Ed.) Adsorption–Desorption Phenomena, Academic Press, London, 1972, p. 391.
[35] G. Federici, D. Holland, J. Brooks, R. Causey, T.J. Dolan, G. Longhurst, in: Proc. 16th IEEE/SOFE, Symp. on Fusion Engineering, Champaign, IL, 30 Sept.–5 Oct., 1995, p. 418.
[36] P. Jung, Fusion Technol. 33 (1998) 63.